

# Dynamics of an Inclusion Complex of Dichloromethane and Cryptophane-E

Zdeněk Tošner,<sup>†,‡</sup> Jan Lang,<sup>§,‡</sup> Dick Sandström,<sup>†</sup> Oleg Petrov,<sup>†</sup> and Jozef Kowalewski<sup>\*,†</sup>

Division of Physical Chemistry, Stockholm University, S-106 91 Stockholm, Sweden, Faculty of Mathematics and Physics, Charles University, Ke Karlovu 3, CZ-121 16 Prague, Czech Republic, and Laboratory of NMR Spectroscopy, Institute of Chemical Technology, Technická 5, CZ-166 28 Prague, Czech Republic

Received: May 4, 2002; In Final Form: July 8, 2002

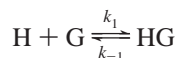
The dynamic properties of the guest–host complex between cryptophane-E and dichloromethane have been studied in tetrachloroethane solution, using proton and carbon-13 NMR, and in the solid state by means of deuterium NMR. The exchange of dichloromethane guest between the free state in the bulk solution and the bound state within the host cavity is slow, on the time scale of seconds, similarly to the earlier studied complex between cryptophane-E and chloroform. The reorientational dynamics of complexed dichloromethane is very fast and is only weakly affected by the reorientation of the guest–host complex as a whole. This result is very different from the case of chloroform inside of the cryptophane cavity. These different pictures of the reorientation of the two chloromethane guests are also nicely reflected in the solid-state deuterium NMR spectra of deuterated guest molecules.

## 1. Introduction

Cryptophanes are known to interact strongly with small neutral species in a hydrophobic environment.<sup>1–9</sup> Cryptophane molecules are globularly shaped and consist of two cyclotri-*tert*-arylene (CTV) units connected by three aliphatic linkers. In the case of cryptophane-E, the linkers are propylene residues. Cryptophanes contain a cavity and can act as hosts accommodating a small guest inside. It has been found that, among a variety of small neutral molecules, cryptophane-E forms a very stable complex with chloroform and a weaker complex with dichloromethane.<sup>10,11</sup> We have recently investigated the dynamics of the inclusion complex between cryptophane-E and chloroform, using carbon-13 and proton NMR spectroscopy in solution, on two different time scales.<sup>12</sup> First, we studied the rate of exchange (slow on the NMR time scale) of the guest between the complexed and free forms. Second, we studied the reorientational dynamics of the guest inside of the host cavity. In the present work, we report a similar investigation of the complex between cryptophane-E and dichloromethane. In addition to the liquid-state NMR measurements, we also present preliminary solid-state deuterium NMR data on the complexes between cryptophane-E and the two chloromethanes. The molecular structure of cryptophane-E and the carbon atom numbering are shown in Figure 1.

## 2. Methods

The complex formation between a host (H) and a guest (G) can be described by a chemical reaction like



where  $k_1$ ,  $k_{-1}$  are reaction rate constants. For the interpretation of NMR experiments, where we can determine the magnetiza-

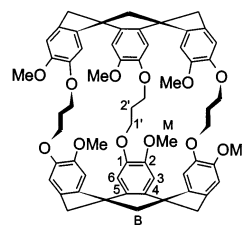


Figure 1. Cryptophane-E.

tion transfer between two different sites, the effective chemical exchange rates are defined as

$$k_{\text{FB}} = [\text{H}]k_1 \quad k_{\text{BF}} = k_{-1}$$

We use a convention where  $k_{\text{FB}}$  is the transfer rate from a free-bulk to a bound-in-complex site, and  $k_{\text{BF}}$  is its counterpart (square brackets denote the molar concentration). The association equilibrium constant is given by the ratio  $k_1/k_{-1}$ .

A careful consideration of the interplay between the chemical exchange according to the scheme above and the nuclear spin relaxation is necessary. Even if the exchange appears slow on the <sup>1</sup>H and <sup>13</sup>C chemical shift scale, it can still be comparable with the time scale of NMR relaxation and can thus influence significantly the apparent relaxation rates of species undergoing the exchange. The sequence of steps, involving several experiments and the use of appropriately modified Bloch equations for the extraction of the longitudinal relaxation times and the heteronuclear steady-state nuclear Overhauser enhancement (NOE) from the relaxation measurements, was presented in our previous work.<sup>12</sup> Here, we only repeat the main ideas.

In the absence of chemical exchange, the <sup>13</sup>C longitudinal relaxation due to the dipole–dipole interaction with the directly bound protons is single exponential, under the conditions of <sup>1</sup>H decoupling. In the presence of exchange between two sites, the modified Bloch equations (see eq 1) can be used to describe the time evolution of the longitudinal nuclear spin magnetizations toward equilibrium.

\* To whom correspondence should be addressed.

<sup>†</sup> Stockholm University.

<sup>‡</sup> Charles University.

<sup>§</sup> Institute of Chemical Technology.

$$\frac{d}{dt} \begin{pmatrix} I_F \\ I_B \end{pmatrix} = \begin{pmatrix} -R_F - k_{FB} & k_{BF} \\ k_{FB} & -R_B - k_{BF} \end{pmatrix} \begin{pmatrix} I_F \\ I_B \end{pmatrix} + \begin{pmatrix} R_F & 0 \\ 0 & R_B \end{pmatrix} \begin{pmatrix} I_F^* \\ I_B^* \end{pmatrix} \quad (1)$$

Equation 1 describes the relaxation of the longitudinal magnetizations  $I_F$  and  $I_B$  that correspond to the  $^{13}\text{C}$  nucleus of  $\text{CH}_2\text{Cl}_2$  in the free (index F) or the bound (index B) states.  $R_F$  and  $R_B$  are the longitudinal relaxation rates ( $R_F = 1/T_{1F}$ ,  $R_B = 1/T_{1B}$ ). The second term in eq 1 yields NOE-enhanced carbon-13 intensities,  $I_F^*$  and  $I_B^*$ , at steady-state in the presence of proton saturation, as they would be if there was no chemical exchange. These intensities are related to the NOE factors at the two sites through  $I_F^* = \text{NOE}_F I_F^0$  and  $I_B^* = \text{NOE}_B I_B^0$ , where  $I_F^0$  and  $I_B^0$  are the equilibrium (unenhanced) carbon magnetizations for the two sites, respectively. We can also write, in the limit when  $t \rightarrow \infty$ , the following relations for calculating the true values of NOE in both sites from a conventional steady-state NOE experiment:

$$\begin{aligned} \text{NOE}_F &= (1 + \eta_F) = \frac{k_{FB} I_F^\infty - k_{BF} I_B^\infty}{R_F I_F^0} + \frac{I_F^\infty}{I_F^0} \\ \text{NOE}_B &= (1 + \eta_B) = \frac{k_{BF} I_B^\infty - k_{FB} I_F^\infty}{R_B I_B^0} + \frac{I_B^\infty}{I_B^0} \end{aligned} \quad (2)$$

The symbols  $I_F^\infty$  and  $I_B^\infty$  are the measured steady-state intensities in the presence of exchange.

The overall strategy one can adopt for deriving the relaxation rates in the free and bound states of dichloromethane is first to determine exchange rates from the proton 1D EXSY-like experiment, second to analyze  $^{13}\text{C}$  inversion recovery data according to eq 1 and by employing the exchange rates measured in the previous step, and third to obtain the NOE parameters from a dynamic NOE experiment using eq 2 and all parameters already determined.

The obvious disadvantage of such a process is the propagation of errors through all the steps to NOE values. The fitting procedure according to eq 1 where the relaxation rates  $R_F$  and  $R_B$  are calculated provides an interesting possibility to verify the consistency of the final output from the processing of all experimental data. The variable parameters used in this second step of the analysis are  $R_F$  and  $R_B$ , of course, but one has to include four more: two intensities of free and bound states at time zero (i.e., immediately after the  $\pi$  pulse in the inversion recovery experiment) and two terms corresponding to the steady-state intensities  $I_F^*$  and  $I_B^*$  introduced in the second term of eq 1. The latter pair of values can be used for cross checking, since the following identity should hold:

$$\frac{I_F^* k_{FB}}{I_B^* k_{BF}} = \frac{\text{NOE}_F}{\text{NOE}_B} \quad (3)$$

Each pair of values in the corresponding ratios is determined on the basis of separated experiments, and thus their inherent mutual correlations are somewhat reduced. One should also note that the left-hand side of eq 3 accumulates uncertainties of four parameters and can be subject to relatively large error.

When the nondipolar mechanisms and the cross-correlation between dipole–dipole interactions are neglected, the longitudinal relaxation time  $T_1$  and NOE factor  $(1 + \eta)$  can be expressed in terms of spectral densities taken at linear combinations of  $^1\text{H}$  and  $^{13}\text{C}$  resonance frequencies<sup>12,13</sup> (see eqs 4–6). The proportionality factor (the square of the dipole–dipole coupling constant,  $b_{\text{CH}}$ ) depends on the sixth power of the CH

distance  $r_{\text{CH}}$ , as well as several universal constants (permeability of vacuum  $\mu_0$ ,  $^{13}\text{C}$  and  $^1\text{H}$  magnetogyric ratios  $\gamma_{\text{C}}$ ,  $\gamma_{\text{H}}$ , and Planck constant  $\hbar$ ).  $N_{\text{H}}$  denotes the number of attached hydrogens.

$$T_1^{-1} = \frac{1}{4} N_{\text{H}} b_{\text{CH}}^2 [J(\omega_{\text{H}} - \omega_{\text{C}}) + 3J(\omega_{\text{C}}) + 6J(\omega_{\text{H}} + \omega_{\text{C}})] \quad (4)$$

$$\begin{aligned} \text{NOE} &= 1 + \eta = \\ &1 + \frac{\gamma_{\text{H}}}{\gamma_{\text{C}}} \frac{6J(\omega_{\text{H}} + \omega_{\text{C}}) - J(\omega_{\text{H}} - \omega_{\text{C}})}{J(\omega_{\text{H}} - \omega_{\text{C}}) + 3J(\omega_{\text{C}}) + 6J(\omega_{\text{H}} + \omega_{\text{C}})} \end{aligned} \quad (5)$$

$$b_{\text{CH}} = -\frac{\mu_0 \gamma_{\text{C}} \gamma_{\text{H}} \hbar}{4\pi r_{\text{CH}}^3} \quad (6)$$

Adopting a certain model of molecular motion, the frequency dependence of the spectral densities can be examined. Lipari and Szabo<sup>14</sup> proposed a simple model assuming isotropic reorientation of the molecule as a whole and a much faster and restricted local motion of individual CH vectors. The two motions are assumed to be uncorrelated; i.e., the corresponding time correlation function can be written as a product  $G(t) = G_{\text{global}}(t)G_{\text{local}}(t)$ . The  $G_{\text{global}}(t)$  depends on a single parameter, the global correlation time  $\tau_{\text{M}}$ , while  $G_{\text{local}}(t)$  is described by two parameters: a generalized order parameter  $S^2$  (defining the degree of restrictions) and the local correlation time  $\tau_{\text{e}}$ . The Lipari–Szabo spectral density has the following form:

$$\begin{aligned} J(\omega) &= \frac{2}{5} \left[ \frac{S^2 \tau_{\text{M}}}{1 + \omega^2 \tau_{\text{M}}^2} + \frac{(1 - S^2) \tau}{1 + \omega^2 \tau^2} \right] \\ \tau^{-1} &= \tau_{\text{M}}^{-1} + \tau_{\text{e}}^{-1} \end{aligned} \quad (7)$$

For a deuterium-labeled guest, deuterium NMR in the solid state can complement the relaxation measurements in solution as a tool for studying motions of the guest inside the host cavity. While detailed predictions of the  $^2\text{H}$  NMR line shapes require a specific motional model, the gross effect of mobility is to narrow the lines.<sup>15</sup> In this report, we limit ourselves to these qualitative and preliminary results.

### 3. Experimental Section

Cryptophane-E (purchased from Acros Chemicals) was first dissolved in nonlabeled dichloromethane in order to remove other possible guests from its cavity. The solvent was then evaporated out and cryptophane-E was dissolved in tetrachloroethane- $d_2$  (Cambridge Isotope Laboratories) in a concentration of 10 mM. For the solution work, the carbon-13-labeled dichloromethane (Cambridge Isotope Laboratories) was added in a 6-fold amount with respect to cryptophane-E, and its final concentration was 59 mM, as determined from the  $^1\text{H}$  NMR spectrum. The sample was degassed by the freeze–pump–thaw procedure (three times) and flame-sealed in a 5 mm NMR tube. For the solid-state experiments, the crystals were grown from solutions of guest molecules, ground to a powder, and transferred to a 5 mm NMR sample holder.

The solution spectra were recorded with a Bruker Avance (11.7 T) spectrometer and with Varian Inova spectrometers (9.4 and 14.1 T) at 273 K. The temperature was calibrated prior to each experimental session, using a standard methanol sample. All of the experiments were repeated at least twice. The peaks of cryptophane-E were assigned in our previous study.<sup>12</sup> The proton signals of  $^{13}\text{CH}_2\text{Cl}_2$  showed splitting with the coupling

constant  $^1J_{\text{CH}} = 178$  Hz in both the free and the bound state. The nonlabeled dichloromethane was found as 25% of the total amount.

The chemical exchange between free and bound dichloromethane sites was measured at two fields (11.7 and 14.1 T) using the DPFGENOE sequence<sup>17</sup> with two shaped hard  $\pi$  pulses (hyperbolic secant) in the mixing period. The selective pulse consisted of a Gaussian cascade<sup>18</sup> covering the spectral area of all three peaks (doublet of  $^{13}\text{CH}_2\text{Cl}_2$  and singlet of  $^{12}\text{CH}_2\text{Cl}_2$ ) of the particular state of dichloromethane. The duration of the selective pulse was 12 ms, and the hard shaped pulses were 350  $\mu\text{s}$  long (the ordinary hard proton  $\pi/2$  pulse was 8  $\mu\text{s}$ ). About 15 different delays were used ranging from 0.05 to 1 s and from 0.05 to 0.3 s when exciting the free and the bound state, respectively. The longest values gave up to 10% of transferred magnetization. The intensity of the excited peak was extrapolated to zero mixing time, and this value was used to normalize the build-up curves for the second peak. These curves were then fitted with a second-order polynomial, and the first derivative at time zero was used as the exchange rate. No carbon decoupling was used during the acquisition period, and the summed intensity of the three lines of the triplet was considered in final processing.

Carbon-13 longitudinal relaxation times  $T_1$  and  $^{13}\text{C}\{-^1\text{H}\}$  steady-state NOE enhancements were measured for both cryptophane and dichloromethane in all three magnetic fields. Since the cryptophane molecule is not very soluble, we had to struggle with sensitivity problems. First, we tried to use a sequence starting with refocused INEPT, followed by a relaxation period with proton decoupling, and with inverse detection (ID) at the end (gradient pulses were used to improve the performance of the sequence).<sup>19</sup> This procedure was tested on the strong  $^{13}\text{CH}_2\text{Cl}_2$  signals with a  $J$ -coupling constant of 178 Hz. The intensity values obtained for short mixing times appeared to be unusually scattered, while the decay for longer times was smooth. The same effect was observed for the cryptophane  $\text{CH}_2$  groups. Analyzing the refocused INEPT for an  $\text{AX}_2$  spin system, one finds that product operators such as  $-C_z - 4H_{1z}H_{2z}C_z$ , i.e., the sum of the one- and three-spin orders, are present at the beginning of the relaxation period. Both of them give rise to the same signal when inversely detected. If we consider proton decoupling as applying pulses and taking an average of product operators over supercycles,<sup>20</sup> then we want to achieve vanishing averages for operators containing the proton part. However, this cannot be done for the three-spin order, because the corresponding operator never changes sign when proton pulses are used. It means that the three-spin order does not vanish because of proton decoupling and will only decay by relaxation. These reasons led us to sacrifice the INEPT enhancement at the beginning of the experiment and replace it with a simple NOE-enhanced scheme. The sequence then becomes an ordinary inversion recovery with inverse detection.<sup>21</sup> The NOE experiments were done in the standard ID manner.<sup>21</sup>

The  $\pi/2$ -pulse durations were 5.7, 8.3, and 7.0  $\mu\text{s}$  for  $^1\text{H}$  and 12.0, 11.8, and 19.6  $\mu\text{s}$  for  $^{13}\text{C}$  in the magnetic fields 9.4, 11.7, and 14.1 T, respectively. The delays for magnetization transfer and refocusing were set to match an  $\text{AX}_2$  spin system with  $^1J_{\text{CH}} = 178$  Hz for dichloromethane and  $^1J_{\text{CH}} = 140$  Hz for cryptophane-E  $\text{CH}_2$  groups. The WALTZ-16 scheme<sup>22</sup> was used for  $^1\text{H}$  decoupling during the relaxation period and NOE build-up at the power level corresponding to a  $^1\text{H}$   $\pi/2$ -pulse  $>150$   $\mu\text{s}$ . During the acquisition period,  $^{13}\text{C}$  decoupling using the GARP scheme<sup>23</sup> was applied (power level corresponding to a  $^{13}\text{C}$   $\pi/2$ -pulse  $>90$   $\mu\text{s}$ ). Fifteen and 10 values of variable delay

in the IR experiment were used, ranging from 0 to 50 s and from 0 to 1 s for dichloromethane and cryptophane, respectively. For NOE measurements, one very short and one very long ( $>10T_1$ ) proton irradiation delay were used. The number of transients was 16 and 3000 for dichloromethane and cryptophane experiments, respectively. The recycle delay was always 5–10 times the longest  $T_1$ . In the case of cryptophane, the relaxation times were determined from peak intensities by three-parameter exponential fitting, and the NOE factor was calculated as the ratio of peak intensities in the two spectra. The bound and free dichloromethane  $^{13}\text{C}$  relaxation times and NOE were determined according to the methods described in the Methods section.

Deuterium solid-state NMR spectra were acquired with a Chemagnetics Infinity spectrometer (9.4 T) employing the quadrupole echo sequence.<sup>16</sup> The  $^2\text{H}$   $\pi/2$  pulse duration was 1.5  $\mu\text{s}$ .

## 4. Results and Discussion

**4.1. Kinetics of the Complex Formation.** Due to the shielding effect of the cyclotrimeratrylene units, the  $^1\text{H}$  resonance of complexed dichloromethane is shifted upfield by 4.26 ppm (free  $\text{CH}_2\text{Cl}_2$  resonates at 5.32 ppm and the bound molecule at 1.06 ppm), and the two sites are in mutual slow exchange on both proton and carbon-13 chemical shift time scales. The  $^1\text{H}$  NMR spectrum at 600 MHz (see Figure 2) also reveals small changes in positions of cryptophane-E resonances upon complexation. The largest shift, when one can see well-resolved peaks, is observed for the line around 4.6 ppm, which corresponds to the  $B_1$  hydrogen in the methylene bridge within the CTV unit. The integration of this spectrum provides, assuming the total concentration of cryptophane-E is 10 mM and using the peak of hydrogens 2' as an internal standard, the following composition of the sample: 8.4 mM cryptophane-E: $\text{CH}_2\text{Cl}_2$  complex (as assessed from the peaks of bound dichloromethane), 50.5 mM free  $\text{CH}_2\text{Cl}_2$ , and 1.6 mM free cryptophane-E. The latter concentration was calculated by subtracting the complex concentration from the total amount of cryptophane-E. This can be roughly checked by direct integration of  $B_1$  peaks, which yields an approximate 2 mM:8 mM ratio of free and complexed cryptophane (the two peaks still overlap, and integration could give distorted results). The equilibrium constant at 273 K can now be determined from the concentrations above to be  $104 \text{ M}^{-1}$  (the literature value<sup>10,11</sup> at 300 K is  $110 \text{ M}^{-1}$ ).

The first step in the analysis of relaxation times of the guest molecule is to determine the effective chemical exchange rates  $k_{\text{FB}}$  and  $k_{\text{BF}}$  of the dichloromethane entering and leaving the host molecule. The DPFGENOE experiment provides spectra of excellent quality, and build-up curves can be obtained with high confidence. The initial build-up (according to the mixing time) of transferred magnetization depends only on a single effective exchange rate,  $k_{\text{FB}}$  or  $k_{\text{BF}}$ , when the free or bound dichloromethane is excited. The effective exchange rates were determined as  $k_{\text{FB}} = 0.032 \text{ s}^{-1} (\pm 0.002 \text{ s}^{-1})$  and  $k_{\text{BF}} = 0.193 \text{ s}^{-1} (\pm 0.007 \text{ s}^{-1})$ ; the error estimates are based on experiments repeated a total of seven times at two magnetic fields. The ratio  $k_{\text{FB}}/k_{\text{BF}} = 0.17$  is in excellent agreement with the ratio of signal integrals of the bound and free states in the  $^1\text{H}$  spectrum (also 0.17). Using the concentration of free cryptophane-E, 1.6 mM, it is possible to evaluate reaction rate constants  $k_1 = k_{\text{FB}}[\text{H}]^{-1} = 20.2 \text{ s}^{-1} \text{ M}^{-1}$  and  $k_{-1} = k_{\text{BF}} = 0.193 \text{ s}^{-1}$ , which can be again used to calculate the equilibrium constant,  $K = k_1/k_{-1} = 105 \text{ M}^{-1}$ , to be compared with  $K$  determined previously, using concentrations ( $104 \text{ M}^{-1}$ ).

Using the DPFGENOE sequence, we were also able to observe weak intermolecular NOE contacts of the bound  $\text{CH}_2\text{Cl}_2$

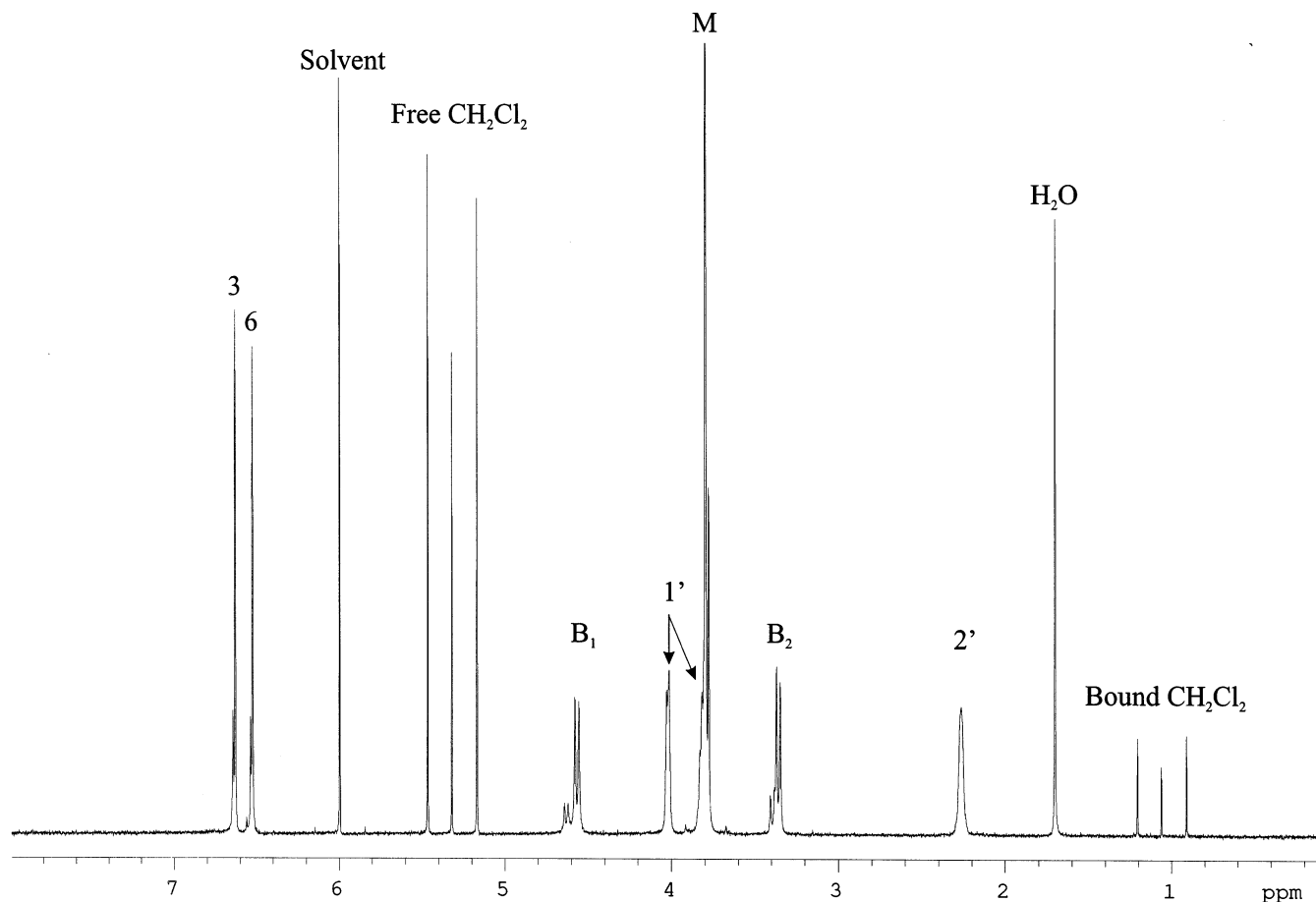


Figure 2. Proton NMR spectrum of cryptophane-E with dichloromethane (14.1 T, 273 K) with assignment.

TABLE 1: Relaxation Parameters Measured for CH<sub>2</sub> Carbons of Cryptophane-E and Dichloromethane Free and Bound in the Complex<sup>a</sup>

carbon	9.4 T		11.7 T		14.1 T	
	$T_1$ , s	NOE	$T_1$ , s	NOE	$T_1$ , s	NOE
B	0.108	1.48	0.140	1.35	0.157	1.25
1'	0.109	1.68	0.147	1.41	0.167	1.27
2'	0.105	1.49	0.142	1.37	0.159	1.23
bound CH <sub>2</sub> Cl <sub>2</sub>	2.71 (0.19)	1.67 (0.18)	3.73 (0.32)	1.55 (0.19)	4.02 (0.30)	1.82 (0.24)
free CH <sub>2</sub> Cl <sub>2</sub>	9.52 (0.24)	2.99 (0.10)	10.03 (0.33)	3.07 (0.10)	10.32 (0.40)	2.88 (0.10)

<sup>a</sup> The numbers in parentheses are standard deviations from the Monte Carlo analysis

protons with its host. The weakness of the signals allows us only a qualitative comparison among interactions with different sites. The dichloromethane molecule interacts mainly with CTV protons (3, 6, M), while the cross-relaxation rate with the propylene linkers is 5–10 times smaller.

**4.2. NMR Relaxation of the Host.** The NMR relaxation of the host molecule was studied in detail in our previous study.<sup>12</sup> However, in the present work we used different experimental conditions (particularly the temperature), so the analysis had to be done again. With the former results at room temperature in mind, we concentrated only on CH<sub>2</sub> carbons denoted as B, 1', and 2' as good markers of the molecular tumbling. The relaxation of these carbons is dominated by the dipolar interaction and is thus suitable for analysis of the molecular dynamics. In the inverse-detected inversion–recovery experiments, we measure predominantly the relaxation of the complexed host, with only a slight contribution from the free form. Considering the composition of the sample and the fact that the presence of the guest is not likely to have a major effect on the host mobility, we simply neglect the effect of the free form

(in addition, the signals of the free form have slightly different chemical shifts for some of the detected protons). The longitudinal relaxation times,  $T_1$ , and the NOEs of the measured carbons are summarized in Table 1.

The fairly spherical shape of the cryptophane-E molecule suggests the model of overall isotropic rotation with restricted local motions to be a reasonable description of its motion. According to this model, we fitted all the relaxation parameters and determined seven variables: the global correlation time  $\tau_M$  and the  $S^2$ ,  $\tau_e$  pairs for all three carbons. The CH distance was taken to be 109.8 pm, as in our earlier relaxation studies.<sup>12,24</sup> The values obtained are shown in Table 2. When the order parameter  $S^2$  is close to unity, then the corresponding local correlation time  $\tau_e$  is very poorly determined and in some of the fits can attain nonphysical, negative values. For this reason, we also used a truncated form of spectral density function (neglecting the second term in eq 7 and thus using only a total of four adjustable parameters) for comparison, which yielded practically unchanged values of the global correlation time and the order parameters. The errors were estimated using a Monte



**TABLE 2: Local Motional Parameters Obtained from the Analysis of Relaxation Data of the Inclusion Complex of Cryptophane-E with CH<sub>2</sub>Cl<sub>2</sub> (the Global Correlation Time is  $\tau_M = 0.97$  ns) and Their Relative Standard Deviations as Obtained from the Monte Carlo Simulation**

carbon	$S^2$	$\Delta S^2$ , %	$\tau_e$ , ps	$\Delta\tau_e$ , %
B	0.77	4	0.01	160
1'	0.72	5	8.8	104
2'	0.76	4	0.01	194
bound CH <sub>2</sub> Cl <sub>2</sub>	0.02	16	1.8	58

Carlo (MC) simulation assuming 5% error in  $T_1$  and 10% in NOE values. Order parameters  $S^2$  about 0.7–0.8 were obtained, in analogy with our previous study, with the chloroform guest at room temperature.<sup>12</sup> The global correlation time of 0.97 ns at 273 K was, as expected, found to be longer than the corresponding value of 0.67 ns measured at 303 K for the chloroform: cryptophane-E case.

**4.3. NMR Relaxation of the Guest.** Because of the chemical exchange between the two sites taking place on a similar time scale as nuclear relaxation, it was necessary to use a more elaborate approach (described above) to extract relaxation times and cross-relaxation constants of the guest from the signal intensities. The first step—the assessment of the exchange rates—is already presented above. In the second step we consider these rates as fixed and plug them into eq 1 in order to fit the time course of signal intensities corresponding to free and bound states of dichloromethane, and thus to determine the relaxation rates  $R_F$  and  $R_B$ . In the last step, all of these values are then employed in eq 2 and the NOE values are calculated.

The drawback of this “step-by-step” approach is that the experimental error of the each step is directly introduced into the next one, and the NOE values accumulate the uncertainties of all the possible sources during the experiments as well as the analysis. The error propagation can be avoided when all the data are adjusted simultaneously in a single fit. However, it can be questioned why exchange data should be included, since they are truly independent of the relaxation of carbon spins. Furthermore, while the relaxation experiments are done at several magnetic fields, this is clearly not necessary for the chemical exchange. Thus, we do not attempt to develop any better approach but use the present one with careful errors estimations based on Monte Carlo (MC) simulations of each computation step.

The relaxation parameters of dichloromethane are given in Table 1 together with the estimated errors. In MC simulations, a variation of measured intensities on a 2–4% level was used, as assessed in repeated experiments. Standard deviations of the exchange rates as described above were also considered, and parameter errors calculated at one step of the analysis were used in the simulations of the following steps. The biexponential nature of relaxation makes it difficult to extract very precise  $T_1$  values, especially if the two are of similar magnitude. This also causes more than two times higher uncertainty of  $R_B$  compared to  $R_F$ . The cross checking condition given by eq 3 yields (left-versus right-hand side)  $2.4 \pm 0.5$  vs  $1.8 \pm 0.3$ ,  $2.1 \pm 0.5$  vs  $2.0 \pm 0.3$ , and  $1.2 \pm 0.2$  vs  $1.6 \pm 0.3$  for the analysis of the experiments at 9.4, 11.7, and 14.1 T, respectively, which only underlines how tricky the biexponential analysis can be.

Despite this quite unfortunate coincidence of the parameter values, we can make the following conclusions. When <sup>13</sup>CH<sub>2</sub>Cl<sub>2</sub> is free in the (C<sub>2</sub>D<sub>2</sub>Cl<sub>4</sub>) solution, its relaxation is clearly in the extreme narrowing regime, with the rate independent of magnetic field and with full or almost full NOE (see Table 1). Although the magnitude of the relaxation rate of the complexed

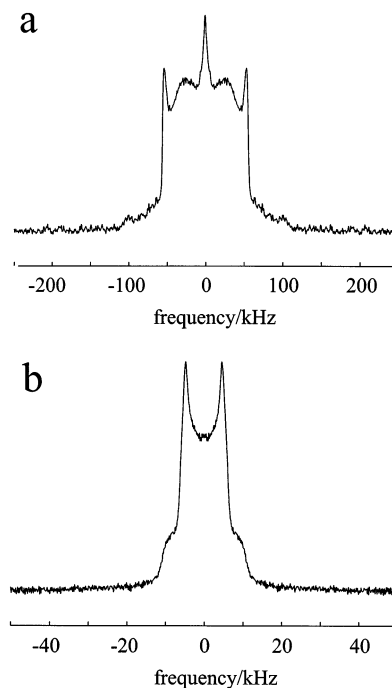


**Figure 3.** <sup>2</sup>H solid-state NMR spectra of the inclusion complexes of cryptophane-E with deuterated chloroform (a) and dichloromethane (b) obtained at 293 K (notice the difference in the frequency scale).

dichloromethane also suggests extreme narrowing, it is important to notice that the rate is slightly field dependent (at least the  $T_1$  at 9.4 T is considerably shorter than the values at higher fields) and that the NOE enhancement is significantly less than full.

One can now speculate about the motional model to use in order to explain such a behavior. We tried to fit the data according to the same model as for the cryptophane-E molecule, assuming the fixed global correlation time  $\tau_M = 0.97$  ns. A reasonable agreement with experiments was obtained with the order parameter  $S^2 = 0.02$  and the local correlation time  $\tau_e = 1.8$  ps (see also Table 2). We interpret these values in terms of the CH<sub>2</sub>Cl<sub>2</sub> molecule tumbling rapidly inside the cryptophane cavity; the motion is almost but not quite isotropic, and the relaxation behavior of dichloromethane also carries the signature of the much slower global motion of the complex. This is in contrast with the case of chloroform, which is almost fixed in the cavity. Using the concept of dynamic coupling,<sup>25</sup> we can say that the motion of dichloromethane is only weakly coupled to the motion of the host, while the coupling is much stronger for chloroform. The difference in the dynamics of the guests can probably be explained by considering their van der Waals sizes—dichloromethane is about 20% smaller and thus has more space to move. Another possible explanation can be sought in the symmetry of the host and the guests and its effect on the guest–host potential: the matching 3-fold symmetry of chloroform and cryptophane-E can perhaps result in a relatively high barrier for the reorientation of the CH bond in this system.

**4.4. Solid-State Deuteron NMR of the Guest.** Deuteron NMR spectra for powder samples of guest–host complexes of cryptophane-E with chloroform and dichloromethane are shown in Figure 3. The spectrum with deuterated chloroform as guest is broad, corresponding to an almost rigid lattice with a quadrupolar coupling constant (QCC) of about 145 kHz. This QCC agrees well with the values of 163–168 kHz obtained at low temperature in solid chloroform.<sup>26,27</sup> These findings are thus consistent with the conclusion from the liquid-state relaxation work<sup>12</sup> that the chloroform guest interacts strongly with the host molecule.

To the contrary, the spectrum of deuterated dichloromethane is much narrower. The QCC for deuterons in dichloromethane at low temperature in solid phase<sup>27,28</sup> is 160–176 kHz, not very different than that in chloroform. Thus, the large line width difference in the solid-state deuteron NMR spectrum cannot depend on the strength of the quadrupolar interaction, but rather on the dynamics of the guest within the host cavity. This is again fully consistent with the present liquid-state carbon-13 relaxation data. The deuteron line shapes from the solid samples of the complexes of cryptophane-E with chloromethanes change with temperature and can be simulated using different models for the motion of the guest molecules within the host cavity. We are planning to present these data in a forthcoming communication.

## 5. Conclusion

The dynamic properties of the complex between cryptophane-E and dichloromethane have been studied in tetrachloroethane solution. The dichloromethane guest exchanges slowly (on a time scale of seconds) between the free state in the bulk solution and the bound state inside the host cavity, similarly to the earlier studied complex between cryptophane-E and chloroform. The reorientational dynamics of complexed dichloromethane, on the other hand, is very different from the dynamics of chloroform inside the cryptophane cavity. While the chloroform guest behaves as an integral part of the molecule, at least on the scale of the rotational correlation time, the reorientation dynamics of the dichloromethane guest is only weakly affected by the reorientation of the guest–host complex as a whole. These different pictures of the guest reorientation are nicely reflected in the solid-state deuteron NMR spectra of deuterated guest molecules.

**Acknowledgment.** This work has been supported through grants from the Swedish Research Council (to J.K. and D.S.), from the Swedish Institute (to O.P. and Z.T.), from Magn. Bergvalls Stiftelse and Carl Tryggers Stiftelse för Vetenskaplig Forskning (to D.S.) and from the Grant Agency of the Czech Republic (No. 203/01/P066 to J.L.).

## References and Notes

- (1) Gokel, G. W. *Large Ring Molecules*; Semlyen, J. A., Ed.; John Wiley & Sons Ltd.: Chichester, 1996; pp 263–307.
- (2) Cram, D. J.; Tanner, M. E.; Keipert, S. J.; Knobler, C. B. *J. Am. Chem. Soc.* **1991**, *113*, 8909.
- (3) Potter, M. J.; Kirchhoff, P. D.; Carlson, H. A.; McCammon, J. A. *J. Comput. Chem.* **1999**, *20*, 956.
- (4) Kobayashi, K.; Asakawa, Y.; Kikuchi, Y.; Toi, H.; Aoyama, Y. *J. Am. Chem. Soc.* **1993**, *115*, 2648.
- (5) Bartik, K.; Luhmer, M.; Dutasta, J. P.; Collet, A.; Reisse, J. *J. Am. Chem. Soc.* **1998**, *120*, 784.
- (6) Brotin, T.; Lesage, A.; Emsley, L.; Collet, A. *J. Am. Chem. Soc.* **2000**, *122*, 1171.
- (7) Luhmer, M.; Goodson, B. M.; Song, Y. Q.; Laws, D. D.; Kaiser, L.; Cyprien, M. C.; Pines, A. *J. Am. Chem. Soc.* **1999**, *121*, 3502.
- (8) Gareil, L.; Dutasta, J. P.; Collet, A. *Angew. Chem., Int. Ed. Engl.* **1993**, *32*, 1169.
- (9) Canceill, J.; Lacombe, L.; Collet, A. *C. R. Acad. Sci., Ser. 2* **1987**, *304*, 815.
- (10) Canceill, J.; Lacombe, L.; Collet, A. *J. Am. Chem. Soc.* **1986**, *108*, 4230.
- (11) Canceill, J.; Cesario, M.; Collet, A.; Guilhem, J.; Lacombe, L.; Lozach, B.; Pascard, C. *Angew. Chem., Int. Ed. Engl.* **1989**, *28*, 1246.
- (12) Lang, J.; Dechter, J. J.; Effemey, M.; Kowalewski, J. *J. Am. Chem. Soc.* **2001**, *123*, 7852.
- (13) Canet, D. *Nuclear Magnetic Resonance: Concepts and Methods*; John Wiley & Sons Ltd.: Chichester, 1996.
- (14) Lipari, G.; Szabo, A. *J. Am. Chem. Soc.* **1982**, *104*, 4546.
- (15) Spiess, H. W. *Adv. Polym. Sci.* **1985**, *66*, 23.
- (16) Davis, J. H.; Jeffrey, K. R.; Bloom, M.; Valic, M. I.; Higgs, T. P. *Chem. Phys. Lett.* **1976**, *42*, 390.
- (17) Stott, K.; Keeler, J.; Van, Q. N.; Shaka, A. J. *J. Magn. Reson.* **1997**, *125*, 302.
- (18) Emsley, L.; Bodenhausen, G. *Chem. Phys. Lett.* **1990**, *165*, 469.
- (19) Dayie, K. T.; Wagner, G. *J. Magn. Reson. A* **1994**, *111*, 121.
- (20) Shaka, A. J.; Keeler, J. *Prog. NMR Spectrosc.* **1987**, *19*, 47.
- (21) Skelton, N. J.; Palmer, A. G.; Akke, M.; Kördel, J.; Rance, M.; Chazin, W. J. *J. Magn. Reson. B* **1993**, *102*, 253.
- (22) Shaka, A. J.; Keeler, J.; Freeman, R. *J. Magn. Reson.* **1983**, *53*, 313.
- (23) Shaka, A. J.; Barker, P. B.; Freeman, R. *J. Magn. Reson.* **1985**, *64*, 547.
- (24) Kowalewski, J.; Mäler, L.; Widmalm, G. *J. Mol. Liq.* **1998**, *78*, 255.
- (25) Behr, J. P.; Lehn, J. M. *J. Am. Chem. Soc.* **1976**, *98*, 1743.
- (26) Ragle, J. L.; Sherk, K. L. *J. Chem. Phys.* **1969**, *50*, 3553.
- (27) Kunwar, A. C.; Gutowsky, H. S.; Oldfield, E. *J. Magn. Reson.* **1985**, *62*, 521.
- (28) Minott, G. L.; Ragle, J. L. *J. Magn. Reson.* **1976**, *21*, 247.